POAC'25
St. John's, Newfoundland and Labrador, Canada

Proceedings of the 28th International Conference on Port and Ocean Engineering under Arctic Conditions
Jul 13-17, 2025
St. John's, Newfoundland and Labrador
Canada

Finite Element Modeling of Effects on ice loading from Collision of Ice Floes with rigid and elastic structures

Yu Chaoge, Tian Yukui*, Wang Weibo, Gang Xuhao, Zhao Weihang
China Ship Science Research Center, Wuxi 214082, China
(*correspondence: tianyukui@cssrc.com.cn）

ABSTRACT

This study presents a comprehensive numerical simulation examining the impact of ice floes with varying shapes and sizes on the ice loading of both rigid and elastic structures. The conventional Drucker–Prager plasticity model, enhanced by the integration of damage mechanics, was employed to accurately represent the material behavior of ice. This model is further coupled with an element erosion technique to investigate the fracture behavior of ice floes upon collision with structural surfaces. The study explores the influence of structural deformation on the characteristics of the ice load.

KEY WORDS : Drucker–Prager model; ice floes; structural deformation; ice loading

INTRODUCTION

In the context of increasingly intense global climate change, the rapid melting of Arctic sea ice and the increase of interannual volatility have made it a key and hotspot area in the field of climate and environmental change research. The increase in the seaworthiness of the Arctic shipping lanes and the exploitation of Arctic resources due to the rapid melting of sea ice in summer will also bring new opportunities and challenges to the global economic development. As a key input in the design and safety assessment of ice structures, ice load has always been a research hotspot with both scientific and engineering significance, and it can be directly used in structural optimization, structural safety assessment, fatigue analysis and structural safety operation early warning. Therefore, the analysis of the time-frequency characteristics and spatio-temporal evolution of structural ice loads can refine the description of the structure-ice interaction process, and comprehensively improve the research level of ice mechanics (Sodhi, 1991; Sodhi, 2001).

At present, the methods for simulating structure-ice interaction mainly include the discrete element method, the finite element method and the PeriDynamics method. When structural deformations are to be considered, the finite element method is the dominant methods. Therefore, the FEM is used for simulation in this paper, and the common methods to describe

the failure of brittle materials in FEM include the cohesive Zone model (CZM), the node splitting technique and the element deletion method.

Konuk first proposed the use of the CZM to simulate the interaction between ice and structure (Konuk, 2009; Konuk,2010). Subsequently, Gürtner used CZM to simulate the interaction between the lighthouse and the sea ice, and compared the simulation results with Full-scale measurements (Gürtner, 2010). With the recognition of the applicability and potential of the cohesive element model in simulating the interaction process between ice and structure, some scholars have begun to study the limitations of the cohesive element model. For example, Pang studied the influence of mesh size and shape on the calculation accuracy of the cohesive element model (Pang, 2015), and concluded that the calculated ice load has a serious mesh dependence, and the smaller the element size, the larger the simulated average ice load. CZM can only simulate cracks between elements. When simulating small-scale cracks, the mesh needs to be fine enough, which will result in expensive time costs. In order to obtain accurate ice loads, it is necessary to give accurate mechanical parameters to the ice material and select the appropriate mesh size. Herrnring developed Mohr-Coulomb Nodal Split (MCNS) ice material model to enable efficient physical based ice-structure interaction simulations. The MCNS model takes spalling and crushing into account, which significantly increases the versatility and reliability of the approach. The confinement effect on the crushing strength and the anisotropic failure behaviour of the ice is modelled by the Mohr-Coulomb material model (Herrnring, 2023).

Ehler and Kujala employed LS-DYNA with a plastic model and element deletion method to simulate ice beam bending failure (Ehlers, 2014), distinguishing tensile and compressive stress-strain relationships. Sazidy applied similar constitutive models and element deletion method to simulate wedge-shaped ice plate bending failures while considering strain rate effects on compressive behavior (Sazidy, 2015). Taylor and Jordaan (Taylor, 2013) used element deletion method to simulate pressure softening and rupture processes. Kim and Jeon used the traditional Drucker–Prager plasticity model and element deletion method to simulate ice-cone and ice-ship interaction, the numerical results of the global ice load are close to the experimental tests (Jeon, 2021, Kim, 2024).

Sum up, the computational efficiency of the CZM and the node splitting technical is low. In this study, the ice follows the Drucker-Prager (DP) plastic model with element deletion method was used.

NUMERICAL MODEL

Ice Constitutive Relationship

Before the damage starts, the mechanical behavior of the material obeys the preset constitutive model, and when the damage starts, the stiffness of the material degrades until the bearing capacity is completely lost, and the element is deleted, which is macroscopically manifested as a crack. In summary, when using the element deletion model, it is necessary to set the constitutive model, the damage initiation criterion and the element failure criterion. In this paper, the pre-damage initiation model follows the Drucker Prager plastic model, which exhibits strain-hardening behavior after yielding, and the material begins to damage and stiffness degrades when the equivalent plastic strain reaches a certain value. The Drucker Prager plastic model introduces the effect of hydrostatic pressure into the Mises yield criterion.

The DP model extends the von Mises criterion by incorporating hydrostatic pressure effects. Three yield surface forms exist (linear, hyperbolic, etc.), as shown in Figure 1(a). The linear form was selected for its ability to accommodate different yield values in triaxial tension/compression through separate dilation (β) and friction angles. The cohesion term (d) and hydrostatic pressure (p) are key parameters. Model selection depends on analysis type, material behavior, experimental data availability, and pressure stress ranges. While hyperbolic DP better matches triaxial test data at low confining pressures, the linear DP model was chosen for parameter calibration convenience using cohesion and friction angle values converted from Mohr-Coulomb parameters.

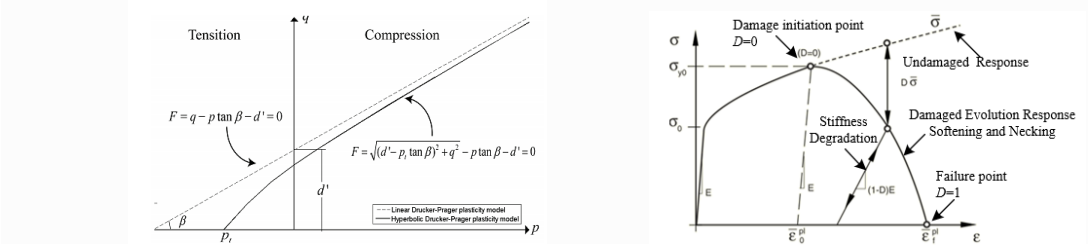

(a) Drucker Prager Plastic model (b) Ductile damage model

Figure 1. Ice Constitutive Relationship

Numerical Model and Parameter Selection

The Finnish-Swedish Ice Class Rules (FSICR) assume ice load distributions on ship hulls as shown in Figure 2, where high-pressure zones concentrate near structural stiffeners. However, Mattanen's mesoscale experiments revealed that high-pressure zones may also occur at mid-span locations, indicating incomplete understanding of structural elastoplastic effects on ice load distribution (Määttänen, 2011). Thus, structural support stiffness effects warrant further investigation.

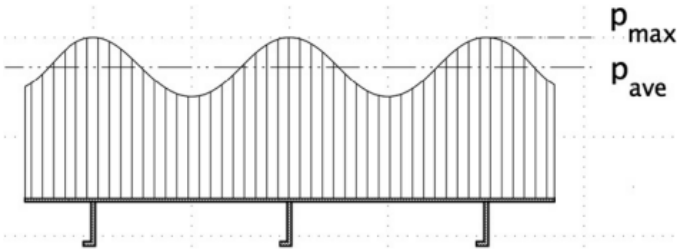

Figure.2 Hull surface pressure distribution assumptions in the code

The numerical simulation considered slow extrusion and high-speed collision scenarios using rigid (10mm thick plate) and elastic models (1m×1m panel with 1.5mm plating and stiffeners. Corresponding numerical models (Figures 3(a)-3(b)) employ shell elements for structures and prismatic hexahedral elements for ice. The numerical model corresponds to the model scale, and the parameters of the sea ice are compared to the model ice in the small ice basin in CSSRC in order to be compared with future experiments. Ice parameters (Table 1) were referenced form the paper of Kim and were calibrated through prior numerical experiments including uniaxial compression and three-point bending tests.

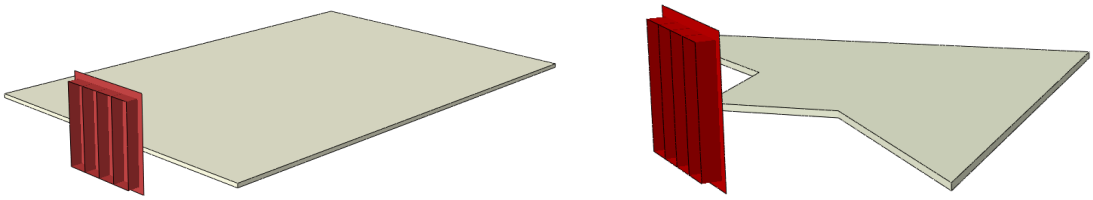

(a) Slow extrusion (b) High-speed collisions

Figure.3 Structural model and corresponding numerical model

Table.1 Sea Ice Material Parameter

Properties of Sea ice			
Density (kg/m^3)	900	Dilation angle (°)	12.0
Young's modulus (MPa)	500	Fracture strain	0.001
Poisson's ratio	0.33	Flow stress ratio	1.0
Friction angle (°)	36.0	Fracture energy (J/m^2)	2.0

NUMERICAL RESULTS

Ice Failure Modes

Numerical simulations covered high-speed collision (0.2-0.8 m/s) and slow extrusion (0.02-0.1 m/s) scenarios for rigid/elastic structures (Table 2). Slow extrusion simulations (Figure 4) showed large ice fragments with combined buckling/extrusion failures, resembling Molikpaq observations. Elastic structures exhibited longer-duration buckling failures compared to rigid counterparts. High-speed impacts (Figure 5) predominantly caused extrusion failures with characteristic load curve signatures.

Table.2 Numerical calculation condition

High-speed collisions		Slow extrusion	
Rigid	Elastic	Rigid	Elastic
	Plate Ribs		
0.8m/s、0.4m/s、0.2m/s		0.1m/s、0.05m/s、0.02m/s	

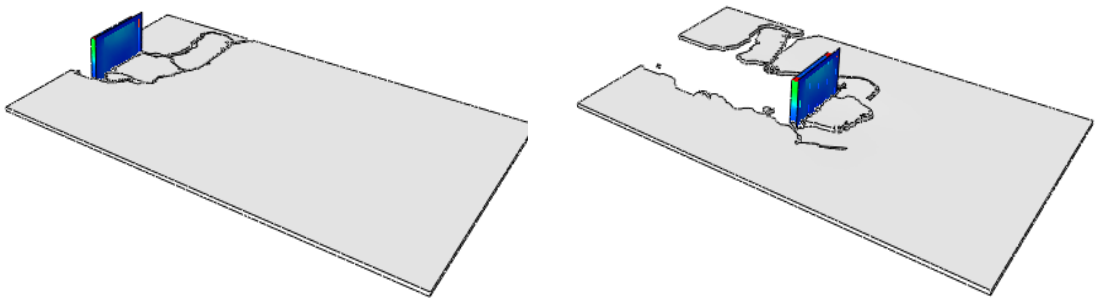

(a) Elastic 10s

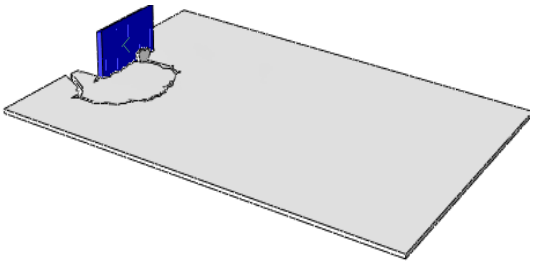

(b) Elastic 30s

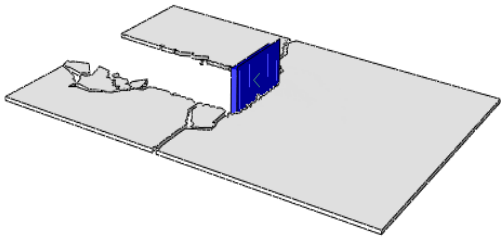

(c) Rigid 10s

(d) Rigid 30s

Figure.4 Failure diagram of sea ice under slow extrusion conditions

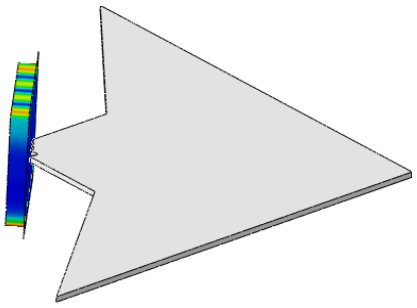

(a) Elastic 1s Ribs

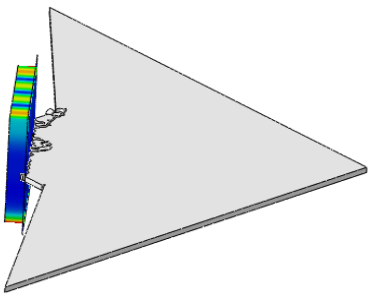

(b) Elastic 3s Ribs

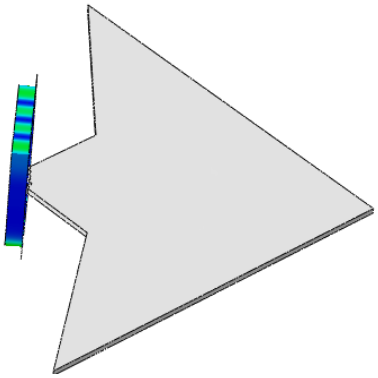

(c) Elastic 1s Plate

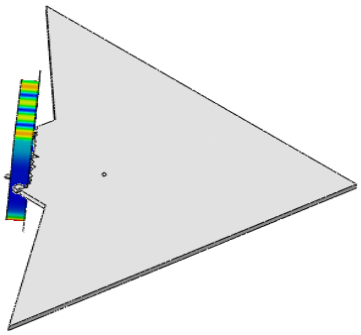

(d) Elastic 3s Plate

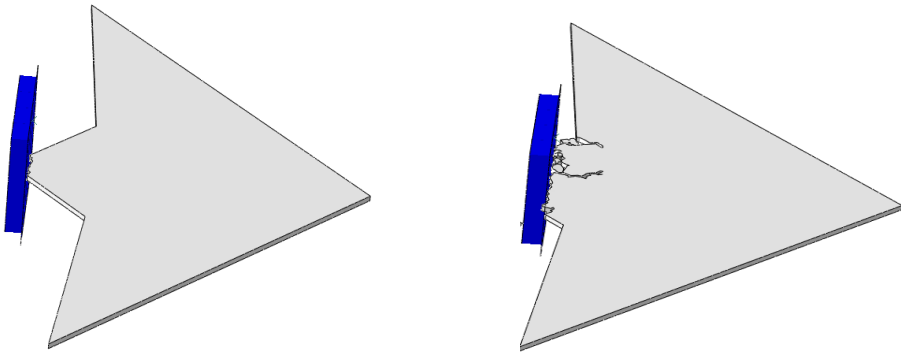

(e) Rigid 1s (f) Rigid 3s

Figure.5 Failure diagram of sea ice under High-speed collisions

Structural Ice Load Analysis

Ice load magnitude and distribution correlate strongly with failure modes and mesh resolution. Slow extrusion simulations (coarser meshes) showed higher ice loads and contact areas for elastic structures, with dynamic high-pressure zones (Figure 7). High-speed impacts (finer meshes) revealed localized load concentrations near stiffeners (Figure 8).

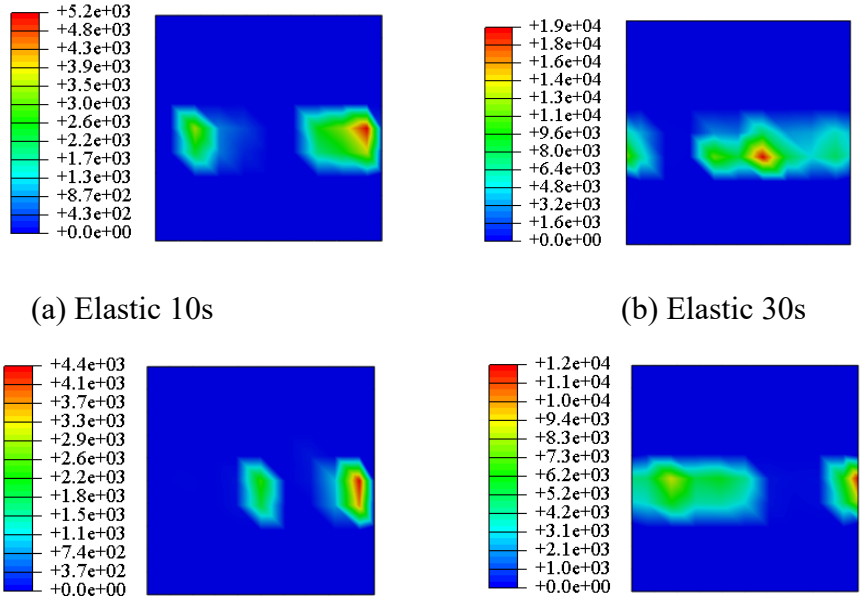

(a) Elastic 10s (b) Elastic 30s

(c) Rigid 10s (d)Rigid 30s

Figure.7 Structural ice load distribution under slow extrusion

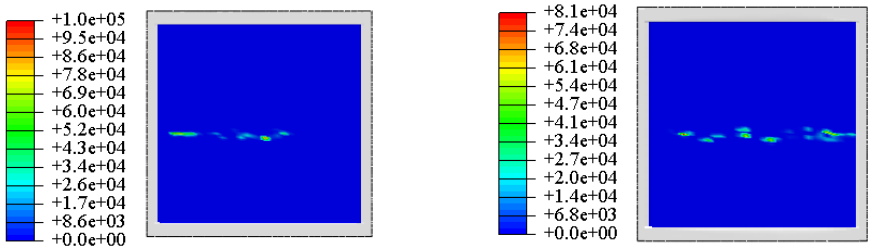

(a) Elastic 1s Plate (b) Elastic 3s Plate

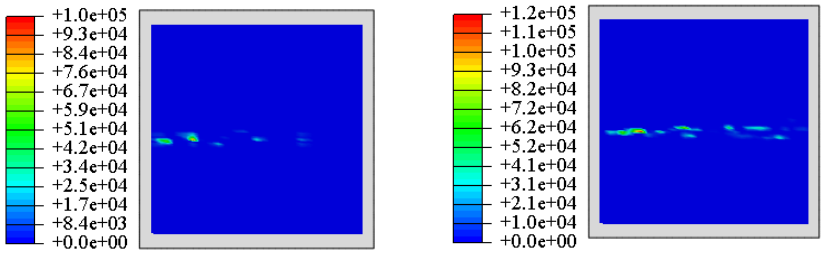

(c)Rigid 0.5s df) Rigid 1s

Figure.8 Structural ice load distribution under High-speed collisions

Time-history comparisons (Figure 9) show elastic structures experience more frequent load drops from buckling events. Average total loads (Figure 10) increase with velocity, being higher for rigid structures in slow extrusion. Conversely, high-speed impacts (Figures 11-12) exhibit higher average loads for elastic structures with significant velocity dependence. Contact area analysis (Figure 13) confirms larger interaction areas for elastic structures across all scenarios.

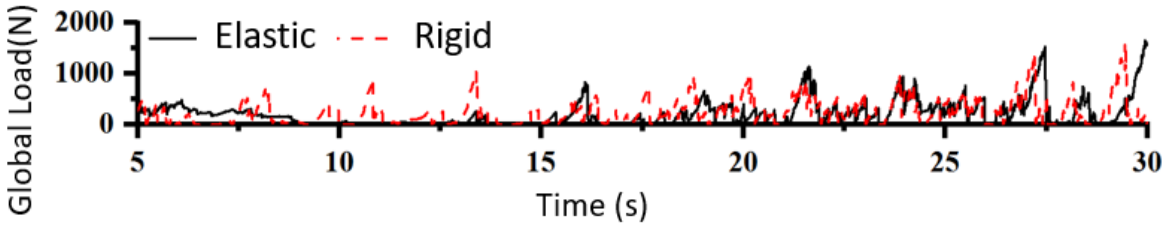

(a) Velocity=0.02m/s

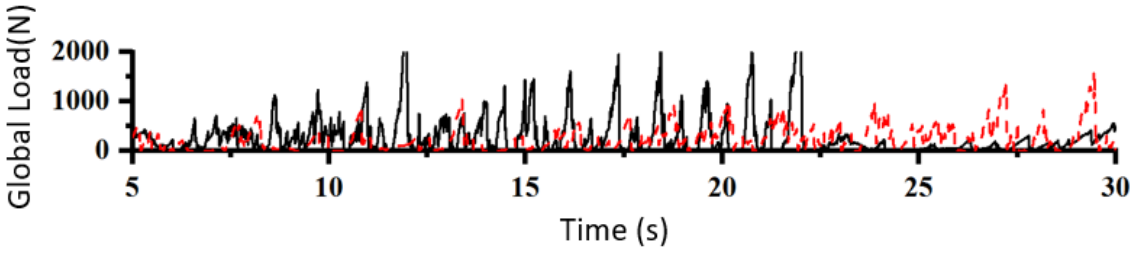

(b) Velocity=0.05m/s

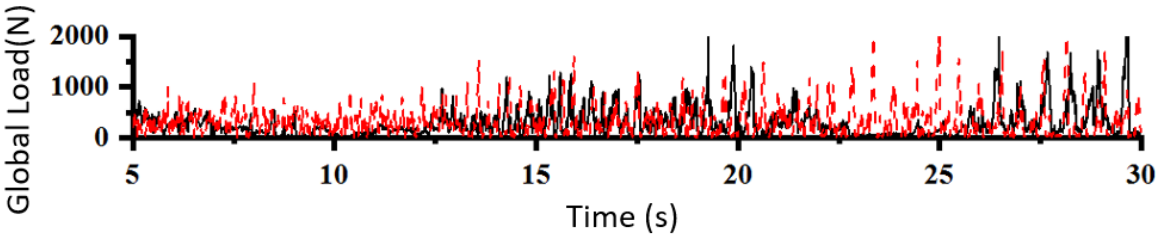

(c) Velocity=0.1m/s

Figure.9 Time history curve of the global ice load under slow extrusion conditions

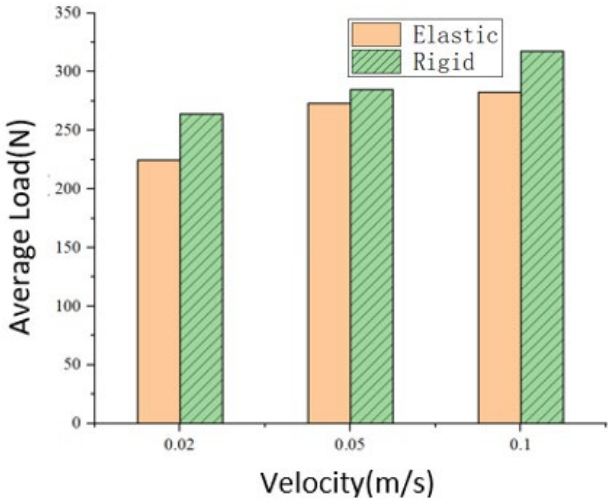

Figure.10 Comparison of the global ice load under the condition of slow extrusion

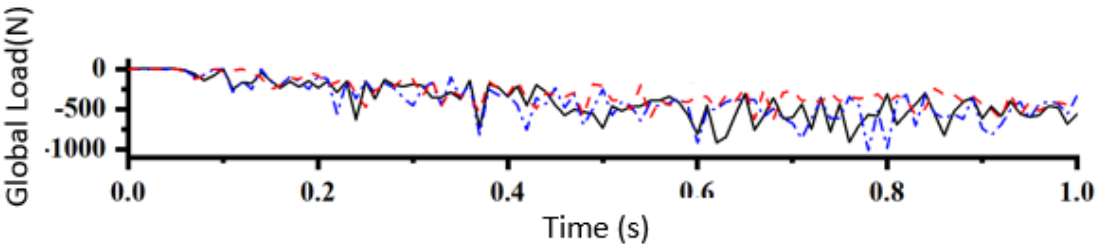

(a) Velocity=0.8m/s

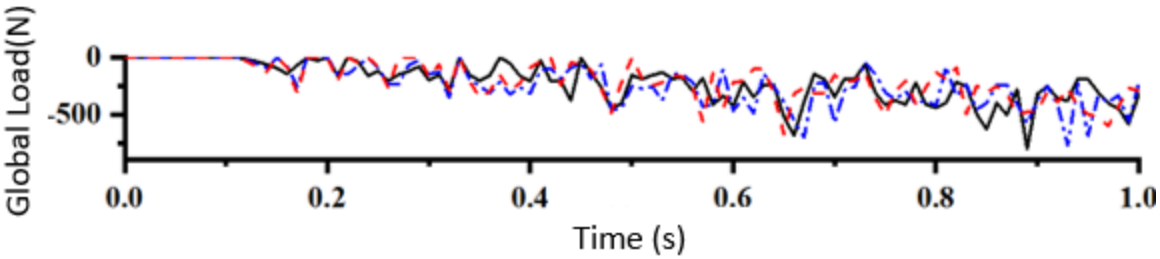

(b) Velocity=0.4m/s

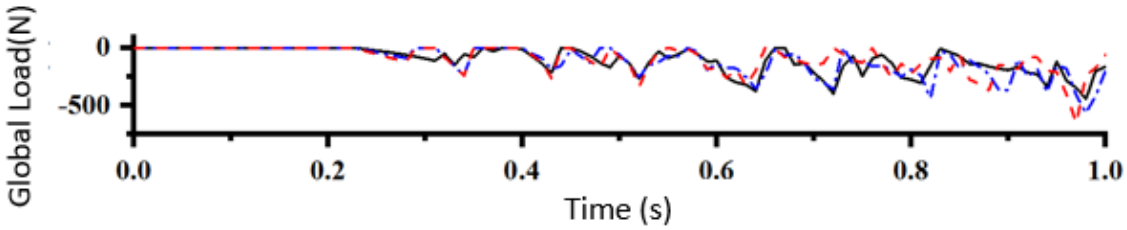

(c) Velocity=0.2m/s

Figure.11 Time history curve of the global ice load under High-speed collisions

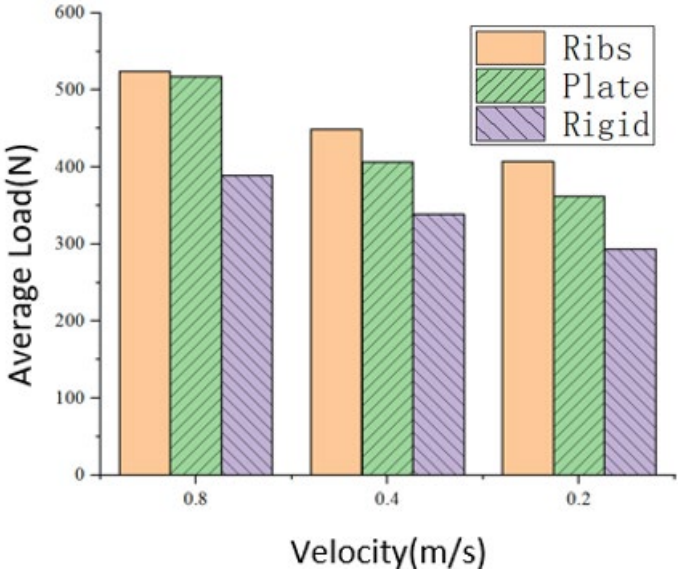

Figure.12 Comparison of the global ice load under the condition of High-speed collisions

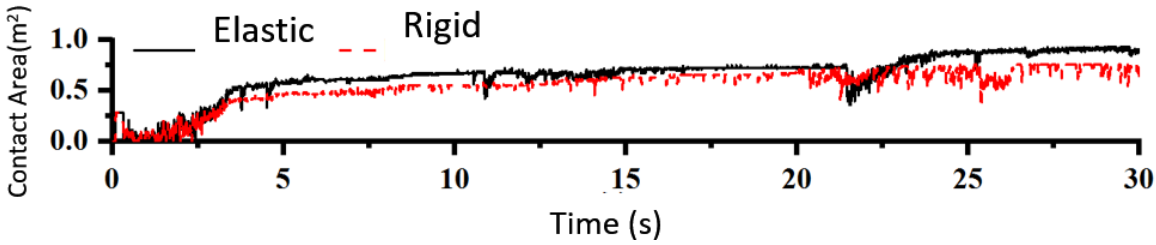

(a) Velocity =0.1m/s，slow extrusion

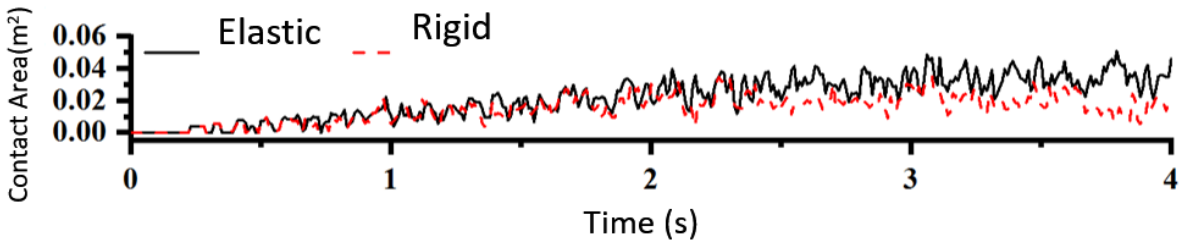

(b) Velocity =0.2m/s，High-speed collisions

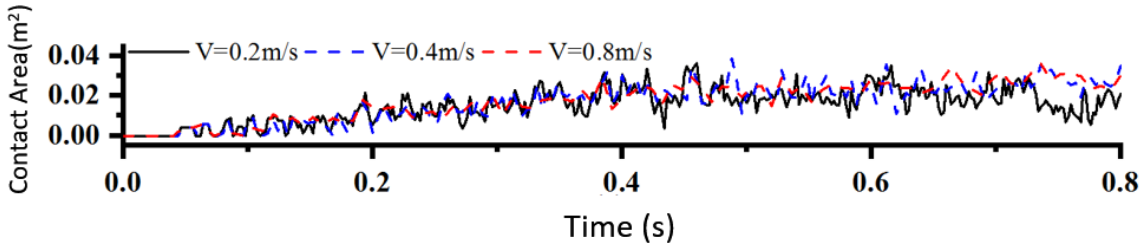

(c) Rigid，High-speed collisions

Figure.13 Contact area and time history curve

CONCLUSIONS

In this paper, a numerical calculation program of structural ice load is established based on the finite element method, and the structural ice load of elastic and rigid structures under the action of slow extrusion and high-velocity collision of sea ice is simulated. Some conclusions are given as follows.

1) Ice load magnitude and distribution correlate strongly with failure modes and mesh resolution. Slow extrusion simulations (coarser meshes) showed higher ice loads and contact areas for elastic structures, with dynamic high-pressure zones. High-speed impacts (finer meshes) revealed localized load concentrations near stiffeners.
2) Elastic structures experience more frequent load drops from buckling events. Average global loads increase with velocity, being higher for rigid structures in slow extrusion.
3) Conversely, high-speed impacts exhibit higher average loads for elastic structures with significant velocity dependence.

ACKNOWLEDGEMENTS

The research sponsored by the National Natural Science Foundation of China (Grant No. G52192690, 52192694).

REFERENCES

Ehlers, S., & Kujala, P. (2014). Optimization-based material parameter identification for the numerical simulation of sea ice in four-point bending. *Journal of Engineering for the Maritime Environment,* 228(1), 70–80.

Gürtner A., Bjerkås M., & Forsberg J. (2010). Numerical Modeling of a Full Scale Ice Event. 20th IAHR Intl. Symposium on Ice, 77-88. Lahti, Finland.

Herrnring, H. J. (2023). Experimental and numerical investigation of brittle ice crushing loads (Doctoral dissertation).

Konuk, I., Gürtner, A., & Yu, S. (2009). A cohesive element framework for dynamic ice-structure interaction problems—Part I: Review and formulation. ASME 2009 28th

International Conference on Ocean, Offshore and Arctic Engineering, 33–41. American Society of Mechanical Engineers.

Konuk, I., Gürtner, A., & Yu, S. (2009). A cohesive element framework for dynamic ice-structure interaction problems—Part II: Implementation. ASME 2009 28th International Conference on Ocean, Offshore and Arctic Engineering, 185–193. American Society of Mechanical Engineers.

Konuk, I., & Yu, S. (2010). A cohesive element framework for dynamic ice-structure interaction problems: Part III—Case studies. ASME 2010 29th International Conference on Ocean, Offshore and Arctic Engineering, 801–809. American Society of Mechanical Engineers.

Määttänen M. (2011). Ice crushing tests with variable structural flexibility. *Cold Regions Science and Technology*, 67: 120-128.

Pang, S. D., Zhang, J., Poh, L. H., et al. (2015). The modelling of ice-structure interaction with cohesive element method: Limitations and challenges. Proceedings of the International Conference on Port and Ocean Engineering Under Arctic Condition

Sazidy, M. S. (2015). *Development of velocity dependent ice flexural failure model and application to safe speed methodology for polar ships*. Ph.D. Memorial University of Newfoundland, Newfoundland, Canada.

Sodhi, D. S. (2001). Crushing failure during ice-structure interaction. *Engineering Fracture Mechanics,* 68, 1889–1921.

Sodhi, D. S. (1991). Ice-structure interaction during indentation tests. *In IUTAM-IAHR Symposium on Ice-Structure Interaction* (pp. 1–15). St. John's, Newfoundland, Canada.

Taylor, R. S., & Jordaan, I. J. (2013). Damage and fracture during contact between a spherical indenter and ice: Experimental results and finite element simulations. *Key Engineering Materials,* 577–578(1), 609–612.

Wells, J., Jordaan, I., Derradji-Aouat, A., & Taylor, R. (2010). Small-scale laboratory experiments on the indentation failure of polycrystalline ice in compression: Main results and pressure distribution. *Cold Regions Science and Technology*, 65(3), 314–325.